Inflammation, Vol. 43, No. 4, August 2020 (© 2020)
DOI: 10.1007/s10753-020-01227-8

ORIGINAL ARTICLE

The Fibroblast-Like Synoviocyte Derived Exosomal Long Non-coding RNA H19 Alleviates Osteoarthritis Progression Through the miR-106b-5p/TIMP2 Axis

Fengjin Tan,[1,3] Dongbo Wang,[1] and Zhongkai Yuan[2]

Abstract—Osteoarthritis (OA) is a common degenerative joint disease that affects people worldwide. The interaction between fibroblast-like synoviocytes (FLSs) and chondrocytes may play a vital role in OA disease pathology. However, the underlying mechanisms by which FLSs exert regulatory effects on chondrocytes still need to be elucidated. Exosomes, small membrane vesicles secreted from living cells, are known to play a variety of roles in mediating cell-to-cell communication through the transferring of biological components such as non-coding RNAs and proteins. Here, we investigate the cellular processes of chondrocytes regulated by FLS-derived exosomes and the mechanisms of action underlying the functions of exosomes in OA pathogenesis. We observed that exosome-mediated cartilage repair was characterized by increased cell viability and migration as well as alleviated matrix degradation. Using chondrocyte cultures, the enhanced cellular proliferation and migration during exosome-mediated cartilage repair was linked to the exosomal lncRNA H19-mediated regulation of the miR-106b-5p/TIMP2 axis. Transfection of miR-106-5p mimics in chondrocytes significantly decreased cell proliferation and migration, promoted matrix degradation characterized by elevated MMP13 and ADAMTS5 expression, and reduced the expression of COL2A1 and ACAN in chondrocytes. Furthermore, we found that TIMP2 was directly regulated by miR-106-5p. Co-transfections of miR-106-5p mimics and TIMP2 resulted in higher levels of COL2A1 and ACAN, but lower levels of MMP13 and ADAMTS5. Together, these observations demonstrated that the lncRNA H19 may promote chondrocyte proliferation and migration and inhibit matrix degradation in OA possibly by targeting the miR-106b-5p/TIMP2 axis. In the future, H19 may serve as a potential therapeutic target for the treatment of OA.

KEY WORDS: Osteoarthritis; Chondrocytes; Exosomes; LncRNA H19; miR-106b-5p.

INTRODUCTION

Osteoarthritis (OA), a noninflammatory chronic joint disorder that is a main cause of disability seen in individuals suffering from arthritis, is characterized by the progressive destruction of joint structures, including both articular cartilage and adjacent tissues [1, 2]. Compelling evidence suggests that synovitis plays a crucial role in the

Fengjin Tan and Dongbo Wang contributed equally to this work.

[1] Orthopedics and Traumatology, Yantai Hospital of Traditional Chinese Medicine, 39, Happy Road, Yantai City, 264000, China
[2] Medical imaging Department, Yantai Hospital of Traditional Chinese Medicine, 39, Happy Road, Yantai City, 264000, China
[3] To whom correspondence should be addressed at Orthopedics and Traumatology, Yantai Hospital of Traditional Chinese Medicine, 39, Happy Road, Yantai City, 264000, China. E-mail: tanfjyhtcm@sina.com

occurrence and progression of OA. Additionally, synovial inflammation is commonly involved in both the early and late stages of OA pathogenesis [3, 4]. Normal synovium is composed of 1 to 3 layers of condensed cells that are mainly fibroblast-like synoviocytes (FLSs) [5]. In normal physiological conditions, FLSs provide nutrients for the articular cartilage and protect joint structures and surrounding musculoskeletal tissue. FLSs also play a role in OA cartilage degradation by producing inflammatory and catabolic factors [6–8]. Some studies demonstrate that FLSs produce a large number of proinflammatory cytokines, such as IL-1β and TNF-α, during OA pathogenesis [9]. Moreover, previous studies have reported that FLSs overexpress multiple enzymes that degrade extracellular matrix (ECM), such as matrix metalloproteinases-13 (MMP13), which plays a crucial role in maintaining cartilage homeostasis. Interestingly, degradation of the ECM is closely associated with OA progression [10]. Chondrocytes, unique cells residing in adult human articular cartilage, maintain cartilage homeostasis through the synthesis of cartilage-specific ECM components and through the balance of anabolic and catabolic pathways. Increasing evidence shows important roles for OA-derived FLSs (OA-FLSs) in cartilage cell proliferation, migration, and apoptosis [11, 12]. A full understanding of the cellular and molecular events in synovial tissues is required to elucidate the pathogenesis of cartilage destruction in OA. Thus, the crosstalk between chondrocytes and FLSs should first be interrogated.

Long non-coding RNAs (lncRNAs), a class of non-protein-coding transcripts larger than 200 nucleotides, are currently recognize as crucial regulators for various biological processes. lncRNAs have the ability to mediate alternative splicing, chromatin modification, gene expression, and RNA metabolism at the epigenetic, transcriptional, and post-transcriptional levels [13]. Several studies have indicated that aberrantly expressed miRNAs and lncRNAs could lead to the deregulated expression of target genes associated with multiple disorders, including OA pathogenesis [14–16]. Recent studies show that miR-30a, miR-449a, and lncRNA-CIR play key roles in ECM degradation and are also involved in OA pathogenesis [17–19]. H19 is one of the well-studied, imprinted maternally expressed lncRNAs. A large number of studies have reported key roles of H19 in numerous cancers, including cancers of the breast [20], liver [21] and bladder [22]. However, only a small number of studies have focused on the roles of H19 in OA pathogenesis. Eric Steck et al. [23] reported that H19 acted as a metabolic correlate in cartilage and cultured chondrocytes *via* regulation of microRNA-675 in osteoarthritis [23].

MicroRNAs (miRNAs) like lncRNAs are another class of RNAs larger than 18–22 nucleotides that do not encode proteins. They function in the regulation of various cell phenotypes, including proliferation, migration, and apoptosis. Recent studies demonstrated that miR-106b-5p plays an important role in the modulation of inflammatory responses [24, 25]. However, the role of lncRNA-H19 in chondrocytes and its contribution to the degradation of the ECM and the pathogenesis of OA have not been fully elucidated.

The goal of this study was to investigate whether lncRNA-H19 participates in phenotypic changes and ECM degradation of chondrocytes through the regulation of miR-106b-5p during OA pathogenesis. To answer our question, we examined expression changes of H19 in both normal and OA cartilage. We also determined how exosomal H19 derived from FLS affected phenotypic changes and the ECM degradation of chondrocytes. Furthermore, the potential mechanisms of H19 were also investigated.

MATERIALS AND METHODS

Patients and Cartilage Specimens

OA cartilage was isolated from the knee joints of 24 OA patients undergoing total knee arthroplasty (13 males, 11 females; age 53–69 years). OA was diagnosed according to the clinical and radiological evaluation criteria published by the American College of Rheumatology (ACR). Normal articular cartilage was obtained from the knees of 10 donors after trauma or death (6 males, 4 females; age 16–48 years). Knee joints of normal cartilage donors exhibited an intact articular surface without signs of cartilage degeneration. Cartilage samples were immediately snap-frozen and stored in liquid nitrogen for further RNA analysis. Informed consent was obtained from all tissue donors. This study was approved by the Human Ethics Committee of Yantai Hospital of Traditional Chinese Medicine. All experiments were performed in accordance with the 1964 Declaration of Helsinki.

Cell Culture

Primary FLSs were isolated from knee joint synovium of newborn SD rats as described previously [5]. Briefly, synovial tissues were rinsed in PBS, minced,

and digested using collagenase type I (Sigma, St. Louis, MO, USA) for 2 h at 37 °C. A cell strainer was then used to filter the cell suspension. After dissociation, cells were centrifuged at 400×*g* for 10 min and maintained in RPMI1640 supplemented with 10% FBS, 100 U/mL penicillin, and 100 μg/mL streptomycin. FLSs were identified as previously described [26] and cells between passages 4 to 8 were used in subsequent studies.

Primary chondrocytes were prepared from the articular cartilages of femoral condyles and tibial plateaus of newborn SD rats as described previously [27]. Briefly, cartilage was washed in PBS before being minced. Minced pieces were then incubated with 3 mg/mL collagenase D for 45 min at 37 °C. After removing the supernatant, cartilage was washed in PBS and incubated with 0.5 mg/mL collagenase D solution overnight at 37 °C. Dissociated cells were filtered through a sterile 48 μm cell strainer and centrifuged for 10 min at 400×*g*. The pellet was resuspended in DMEM supplemented with 10% FBS, 100 U/mL penicillin, and 100 μg/mL streptomycin. The cells were cultured at 37 °C, 5% CO_2 until further analysis.

Cell Transfections

All H19 siRNAs (si-H19; 100 nM), a negative control siRNA (si-NC; 100 nM), an H19-overexpression plasmid (pcDNA3.1-H19), a pcDNA3.1 plasmid, a miR-130a-3p mimic (100 nM), a miR-130a-3p inhibitor (100 nM), and their negative controls (100 nM) were designed and purchased from RiboBio (Guangzhou, China). The sequences of H19-siRNA1#, H19-siRNA2#, and H19-siRNA3# were 5′-UGUAAAGUGCAGCAUAUUCAU-3′, 5′-GAAUAUGCUGCACUUUACAAC-3′, and 5′-UGCAAAUUAAAUUCAGAAGGG-3′, respectively. The sequence of si-NC was 5′-UUCUCCGAACGUGUCACGUTT-3′. The sequences for miR-106b-5p mimic, miR-106b-5p inhibitor, and miR-NC were 5′-UAGACGUGACAGUCGUGAAAU-3′, 5′-GCUGCACUGUCAGCACUUUA-3′, and 5′-UUCUCCGAACGUGUCACGUTT-3′, respectively. Lipofectamine® 2000 (Invitrogen) was used for cell transfections according to the manufacturer's protocol. FLSs were used in experiments after 48 h of transfection.

FLS/Chondrocyte Co-culture

FLSs transfected with pcDNA3.1-H19, pcDNA3.1, si-H19, and si-NC-transfected or treated with GW4869 (5×10^5/well) were placed into the upper chamber of a co-culture system containing a 0.4 μm pore membrane. Chondrocytes (3×10^5/well) were seeded into the lower chamber. All cells were incubated in RPMI-1640 medium supplemented with 10% exosome-free FBS.

Exosomes Isolation and Characterization

Exosomes were isolated from conditioned medium of FLSs using an ExoQuick-TC Kit (System Biosciences, USA). Both nanosight particle tracking analysis (NTA) and transmission electron microscopy (TEM) were used to characterize exosomes.

For exosome uptake analysis, exosomes were labeled with PKH26 Red (PKH26 Red Fluorescent Cell Linker Kits, Sigma-Aldrich) by following manufacturer's instructions. Exosomes were then washed in 10 ml of PBS before the labeled-exosomes were collected by ultracentrifugation and resuspended in PBS. Lastly, 2 μg of exosomes was incubated with 2×10^5 chondrocytes for 48 h, and nuclei were counterstained with 4′,6-diamidino-2-phenylindole (DAPI). Cells were examined under a confocal microscope (Leica, USA).

Cell Proliferation

The effects of FLS-derived exosomes on the proliferation of chondrocytes were measured using a CCK-8 assay. Briefly, 2×10^4 cells/well chondrocytes were seeded into 48-well plates and incubated with various exosomes for 24, 48, and 72 h. Then, 10 μL of CCK-8 was added to each well and maintained for 2 h at 37 °C. Values at an absorbance value of 450 nm were recorded.

Transwell Assays

A transwell assay was used to assess the effects of FLS-derived exosomes on the migration of chondrocytes. Briefly, 5×10^4 chondrocytes were seeded into the upper chamber of a 24-well transwell plate (8-μm-pore-size, Corning). Next, 600 μL of DMEM containing exosomes was added into the lower chamber of the transwell plate and maintained for 24 h at 37 °C. Cells not migrating to the lower surface of the upper chamber were removed using a cotton swab. The upper chamber was then fixed with 4% PFA for 10 min and stained with 0.1% crystal violet for 15 min. Four random fields (× 100 magnification) per well were photographed and counted under an inverted microscope.

Quantitative Real-Time PCR (qRT-PCR)

Total RNA was extracted from cells and tissues using the TRIzol reagent (Invitrogen) following manufacturer's instructions. For miRNAs and U6, synthesis of cDNA was

performed using Mir-X™ miRNA First-Strand Synthesis Kit (Takara, Japan). For mRNAs and GAPDH, reverse transcription was performed using a cDNA Reverse Transcription Kit (Takara). SYBR Green PCR Master Mix (Invitrogen, USA) was used to perform qRT-PCR that was ran using a prism 7500 real-time PCR system (Applied Biosystems, USA). To calculate relative expression levels of specific transcripts, the $2^{-\Delta\Delta CT}$ method was used. Both U6 and GAPDH were used as endogenous controls for miRNA and mRNA, respectively. Primer sequences are as follows: miR-106b-5p: forward: 5′-ACAC TCCAGCTGGGUAGACGUGACAGUCG-3′; reverse: 5′-TGGTGTCGTGGAGTCG-3′. U6: forward: 5′-CAGT GCGTGTCGTGGAGT-3′; reverse: 5′-AACG CTTCACGAATTTGCGT-3′. H19: forward: 5′-AGTG TCCCATTCTTTGGAT-3′; reverse: 5′-CTTG CATAGCACATGAATAT-3′. GAPDH: forward: 5′-GGAGCGAGATCCCTCCAAAAT-3′; and reverse: 5′-GGCTGTTGTCATACTTCTCATGG-3′.

Quantification of Sulfated Glycosaminoglycan

Chondrocytes were dissociated using proteinase K digestion buffer at 65 °C for 3 h. The concentrations of sulfated glycosaminoglycans (sGAG) were measured using the Blyscan Sulfated Glycosaminoglycan Assay Kit (Biocolor Ltd., Carrickfergus, UK) following manufacturer's instructions. Absorbance at 656 nm was determined using a microplate reader (SpectraMax M2, Molecular Devices, LLC, Sunnyvale, USA). A shark chondroitin 6-sulfate (Sigma) was used as the standard. Total sGAG levels were normalized to total dsDNA content.

Western Blotting

Total protein was extracted from cells using radioimmunoprecipitation assay (RIPA) lysis buffer and was quantified using a BCA Protein Assay Kit (Beyotime, China). After separating proteins using SDS-PAGE, equivalent protein concentration was transferred onto polyvinylidene difluoride (PVDF) membranes and then blocked in 5% non-fat milk diluted in Tris-buffered saline with Tween-20 (TBST) for 1 h at room temperature. Subsequently, membranes were incubated with primary antibodies overnight at 4 °C, followed by an extensive wash in TBST. After washing in TBST, membranes were incubated in specific horseradish peroxidase-conjugated secondary antibodies (1:10,000; Cell Signaling Technology, Inc.) for 1 h at room temperature. Enhanced chemiluminescence reaction was used to detect protein bands. Primary antibodies specific to TSG101 (1:200; Santa Cruz Biotech, Dallas, TX, USA), CD63 (1:200; Santa Cruz), COL2A1 (1:200; Abcam, Cambridge, MA, USA), MMP13 (1:200, Santa Cruz, USA), TIMP2 (1:200, Santa Cruz, USA), and GAPDH (1:1000; Beyotime) were used. GAPDH served as an endogenous loading control.

Luciferase Reporter Assays

Wide-type (H19-Wt) and mutant H19 (H19-Mut), where H19-Mut contains mutations in putative miR-106b-5p-binding sites, were inserted into a pmirGLO dual-luciferase reporter vector (Promega, Madison, USA). Similarly, a fragment of the TIMP2 3′-untranslated region (3′ UTR) containing the miR-106b-5p binding site (TIMP2-Wt) and its mutant (TIMP2-Mut) were cloned into the pmirGLO reporter vector. Chondrocytes were co-transfected with pmirGLO-H19-Wt, pmirGLO-H19-Mut, pmirGLO-TIMP2-Wt, pmirGLO-TIMP2-Mut or pmirGLO vector, and a miR-106b-5p mimic or miR-NC control. Renilla luciferase activities of cell lysates were measured using Dual Luciferase Reporter Assay kit (Promega) in accordance with the manufacturer's instructions 24 h after transfection.

Statistical Analysis

All data were presented as mean ± SD. The SPSS 17.0 software was used for statistical analyses. All *in vitro* experiments were independently repeated in triplicates for each experiment. Gaussian distribution, Student's *t* test, or ANOVA statistical analyses were performed. A Mann-Whitney test was performed for non-normal data. A $P < 0.05$ indicated statistically significant differences.

RESULTS

LncRNA H19 Is Downregulated in the Cartilage of OA Patients

To explore whether lncRNA H19 expression was altered in OA compared with normal tissues, qRT-PCR was performed to determine H19 expression levels in both OA and healthy cartilage samples. Data revealed that H19 levels were significantly downregulated in OA patients when compared with the normal control group ($P < 0.01$, Fig. 1a). IL-1β is recognized as one of main cytokines involved in OA progression [28]. Several studies have reported that IL-1β can inhibit cell proliferation, downregulate aggrecan and collagen type II synthesis, and increase MMP13 expression in chondrocytes [29]. Thus, we

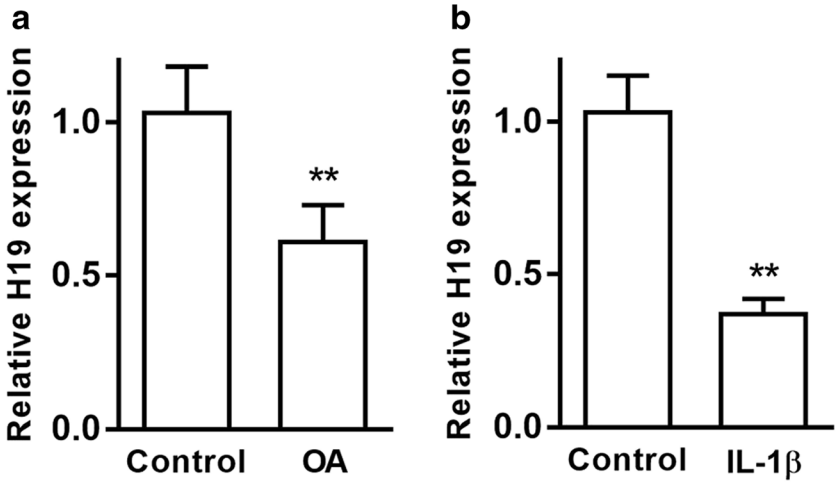

Fig. 1. Relative expression level of H19 in normal and osteoarthritis (OA) cartilage samples detected by qRT-PCR. $^{**}P < 0.01$ compared with the control group

determined the expression levels of H19 in Il-1β-stimulated chondrocytes *in vitro*. As expected, the expression levels of H19 were significantly decreased in chondrocytes treated with IL-1β ($P < 0.01$, Fig. 1b).

FLSs Overexpressing H19 Regulate the Proliferation and Migration of Chondrocytes

To determine whether FLSs favorably contribute to the reversal of IL-1β-induced chondrocytes injury, H19 was overexpressed (FLSs-H19) or suppressed (FLSs-siH19) in FLSs and was co-cultured with chondrocytes that were pre-stimulated with IL-1β (10 ng/mL for 24 h) in a transwell system. After co-culturing for 24 h, chondrocyte proliferation was measured using a CCK-8 assay. It was found that proliferation was significantly suppressed in chondrocytes co-cultured with FLSs-siH19 and was increased in cells co-cultured with FLSs-H19, compared with corresponding controls ($P < 0.01$, Fig. 2a, b). Similarly, using a Boyden chamber transwell system, we observed that the number of migrated chondrocytes decreased when co-cultured with FLSs-siH19. In contrast, this number was increased when co-cultured with FLSs-H19, compared with corresponding controls ($P < 0.01$, Fig. 2c). Altogether, these results provide strong evidence that FLSs overexpressing H19 exerts positive effects on reversing IL-1β-induced chondrocyte injury, suggesting a crosstalk between FLSs and chondrocytes during OA progression.

H19 Is Transferred from FLSs to Chondrocytes Through Exosomes

GW4869 is an inhibitor used to block exosome secretion. We first determined whether GW4869 could successfully block exosome secretion in FLSs-H19. We identified that the FLSs-H19-induced positive effects on chondrocyte proliferation and migration were abolished in the presence of GW-4869 (Fig. 3a, b). These data suggest that FLS-derived exosomes may play a crucial role in the mutual effects observed between FLSs and chondrocytes.

To further confirm whether FLS-derived exosomes (exos-FLS) were involved in the phenotypic changes of chondrocytes, we first isolated exosomes from the conditioned medium of FLSs. Isolated exosomes displayed as small round vesicles with a diameter ranging from 30 to 100 nm and expressed exosomal markers including CD9, CD63, and CD81 (Fig. 3c–e). Importantly, when equal amounts of exosomal protein were loaded, levels of the exosomal markers TSG101 and CD63 were similar in exosomes derived from FLSs-H19 (exos-FLS-H19), FLSs-siH19 (exos-FLS-siH19), and FLSs (exos-FLS) (Fig. 3e), indicating that H19 did not alter exosome secretion by FLSs. To evaluate whether exos-FLS could enter chondrocytes, chondrocytes were incubated with PKH67-labeled exos-FLS. Confocal microscopy showed that the majority of chondrocytes absorbed dye-labeled FLSs-derived exosomes (Fig. 3f). Accordingly, H19 levels were increased in chondrocytes treated with exos-FLS-H19,

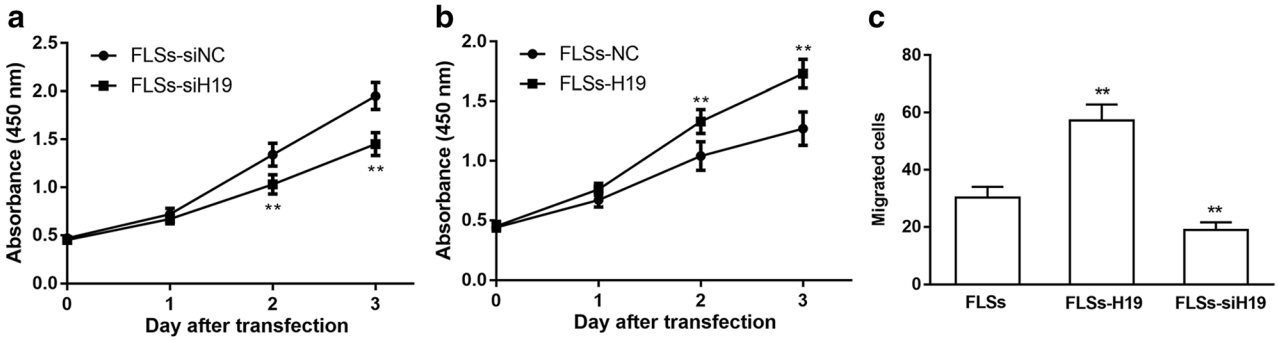

Fig. 2. Viability and migration of chondrocytes are promoted when co-cultured with FLSs overexpressing H19, whereas they are inhibited when co-cultured with FLSs silencing H19. **a** and **b** FLSs overexpressing H19 promoted chondrocytes viability detected by CCK-8 assay (**a**), which was inhibited by FLSs silencing H19 (**b**). **c** The quantitative results of chondrocytes migration determined by transwell experiment are shown. $*P < 0.05$, $**P < 0.01$, compared with the control group

compared with exos-FLS-treated cells. In addition, H19 levels were markedly reduced in chondrocytes incubated with exos-FLS-siH19 compared with exos-FLS-treated cells ($P < 0.01$, Fig. 3g). Collectively, these results indicate that exosomes derived from FLSs can effectively be absorbed and transferred to H19 to chondrocyte cells.

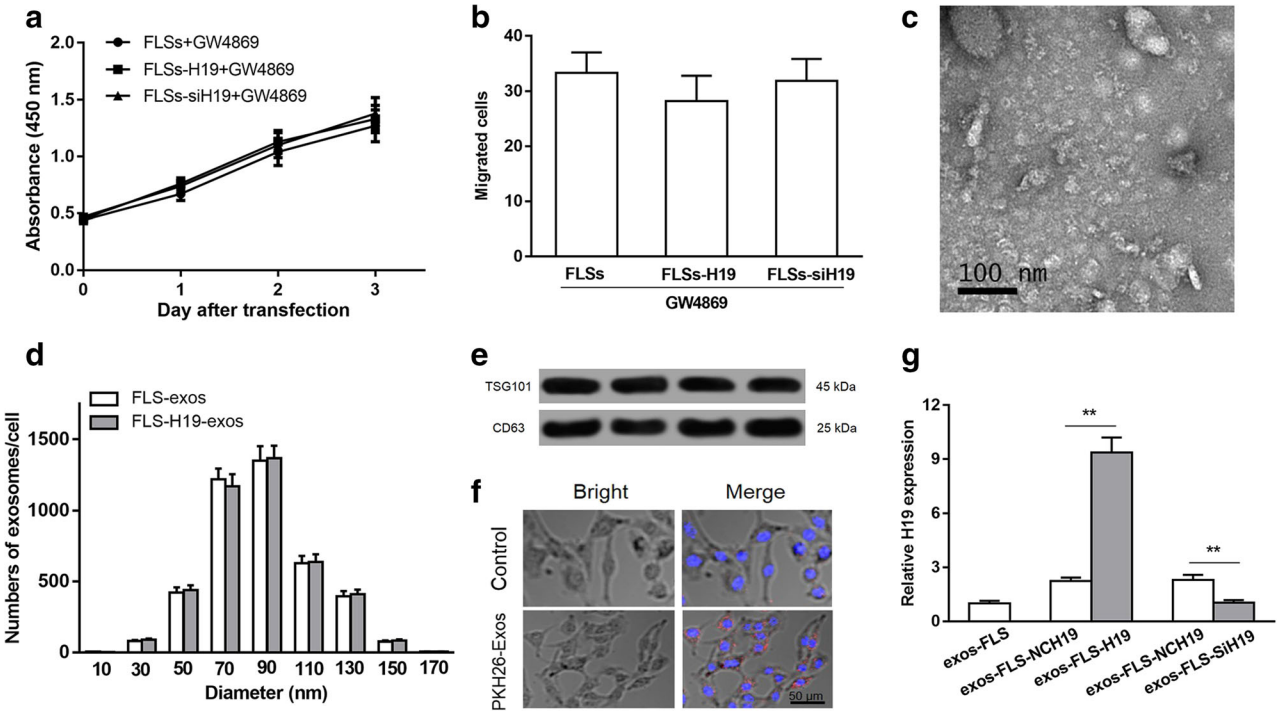

Fig. 3. H19 is transferred from FLS to chondrocytes through exosomes. **a** and **b** FLS-mediated regulatory effects on chondrocytes viability and migration were blocked upon addition of GW4869. **c** Exosomes derived from FLSs were examined under electron microscopy. **d** The size distributions of exosomes derived from FLSs were analyzed by nanoparticle tracking assay. **e** Western blot analysis for exosomal marker TSG101 and CD63 of exosomes derived from FLSs. **f** The uptake of the PKH26 labeled FLS-exos was evident in chondrocytes after 12 h of incubation. No stain was observed in the negative control condition. (scale bar, 50 μm). **g** qRT-PCR detection of H19 in chondrocytes co-cultured with exosomes from FLSs, FLS-H19, and FLS-siH19. $*P < 0.05$, $**P < 0.01$, compared with the control group

Exos-FLS-H19 Treatment Alters the Expression of ECM Degeneration Proteins in Articular Chondrocytes

One of the major causes of cartilage degeneration is the disturbance of extracellular matrix (ECM) anabolism and catabolism in articular chondrocytes. In this study, chondrocytes were pre-stimulated with 10 ng/mL IL-1β for 24 h to mimic OA chondrocytes. An increased production of MMP13 and ADAMTS5 expression levels and a downregulation of COL2A1 (collagen type 2 A1) and ACAN (aggrecan) levels were observed in chondrocytes treated with IL-1β. Exosomes derived from FLSs-H19 (exos-FLS-H19) abolished negative effects of IL-1β on chondrocytes, which was revealed by expression changes in MMP13, ADAMTS5, COL2A1, and ACAN levels ($P < 0.01$, Fig. 4a, b). Immunoblotting analysis was used to examine the expression levels of MMP13 and COL2A1. MMP13 expression was significantly upregulated by IL-1β treatment and downregulated by exos-FLS-H19 (Fig. 4c). In contrast, COL2A1 was significantly reduced by IL-1β stimulation and elevated by exos-FLS-H19 treatment (Fig. 4c). A DMMB assay was used to evaluate the concentration of sGAG, which is a main form of aggrecan secreted by chondrocytes. IL-1β stimulation reduced the concentration of sGAG, but exos-FLS-H19 treatment rescued this effect ($P < 0.01$, Fig. 4d). Collectively, these findings revealed that H19 exhibits protective roles in chondrocyte ECM homeostasis.

H19 Regulates the Proliferation, Migration, and ECM Degradation of Chondrocytes *via* miR-106b-5p

We next questioned the underlying mechanisms behind how H19 exerts a chondroprotective role on OA progression. First, the online software StarBase v2.0 was interrogated and found that miR-106b-5p potentially interacted with H19. As shown in Fig. 5a, compared with control groups, the expression levels of miR-106b-5p were significantly ($P < 0.01$) upregulated in OA articular cartilage. We next examined the expression levels of miR-106b-5p after overexpressing and silencing H19 in chondrocytes. We found that miR-106b-5p levels were decreased in H19 overexpressing chondrocytes. However, these levels were increased when H19 levels were repressed (Fig. 5b). Thus, miR-106b-5p was selected for subsequent studies. To verify that there was a direct interaction between H19 and miR-106b-5p, a luciferase reporter gene system was applied. Co-transfection of H19-Wt and a miR-106b-5p mimic into chondrocytes significantly reduced luciferase activity compared with cells co-transfected with H19-Wt and miR-NC. However, there was no significant difference in luciferase activity when analyzing cells transfected with H19-Mut plasmids (Fig. 5b). Altogether, these data suggest that H19 and miR-106b-5p have a negative regulatory relationship.

We next wanted to determine whether H19 exerts favorable effects reversing IL-1β-induced phenotypic changes of chondrocytes by targeting miR-106b-5p. H19 overexpression significantly ($P < 0.01$) reduced the levels of miR-106b-5p in chondrocytes (Fig. 5c). A miR-106b-5p mimic, pcDNA3.1-H19, and corresponding controls (negative control and vector) were co-transfected into chondrocytes that were then stimulated with IL-1β. A transwell assay was used to determine the effects of H19 and miR-106b-5p on cell migration. The number of migrating cells in the vector/miR-106b-5p mimic group was much lower than what was observed in the vector/negative control group. However, the number of migrating cells was elevated in the pcDNA3.1-H19 group (Fig. 5d). Similarly, CCK8 results revealed that the vector/miR-106b-5p mimic group exhibited decreased proliferation as compared with that the vector/negative control group. The proliferation of chondrocytes was rescued after pcDNA3.1-H19 transfection (Fig. 5e). To examine whether H19 protects ECM from degradation by targeting miR-106b-5p, the expression levels of MMP13, ADAMTS5, COL2A1, and ACAN were determined in miR-106b-5p mimic and pcDNA3.1-H19 transfected chondrocytes. The mRNA levels of MMP13 and ADAMTS5 were significantly upregulated, and the mRNA levels of COL2A1 and ACAN were markedly downregulated in the vector/miR-106b-5p mimic group when compared with the vector/negative control group ($P < 0.01$, Fig. 5f). In addition, the expression levels of MMP13 and ADAMTS5 were decreased, whereas COL2A1 and ACAN were elevated after the addition of pcDNA3.1-H19 ($P < 0.01$, Fig. 5g). In summary, these results demonstrated that H19 inhibited Il-1β-induced negative phenotypic changes of chondrocytes and ECM degradation through miR-106b-5p.

TIMP2 Is Repressed by miR-106b-5p in Chondrocytes

A positive correlation between TIMP2 expression and H19 expression ($r = 0.537$, $P < 0.01$) and a negative correlation ($r = -0.637$, $P < 0.01$) between TIMP2 expression and miR-106b-5p expression levels were observed in OA cartilage samples. Overexpressed H19 and

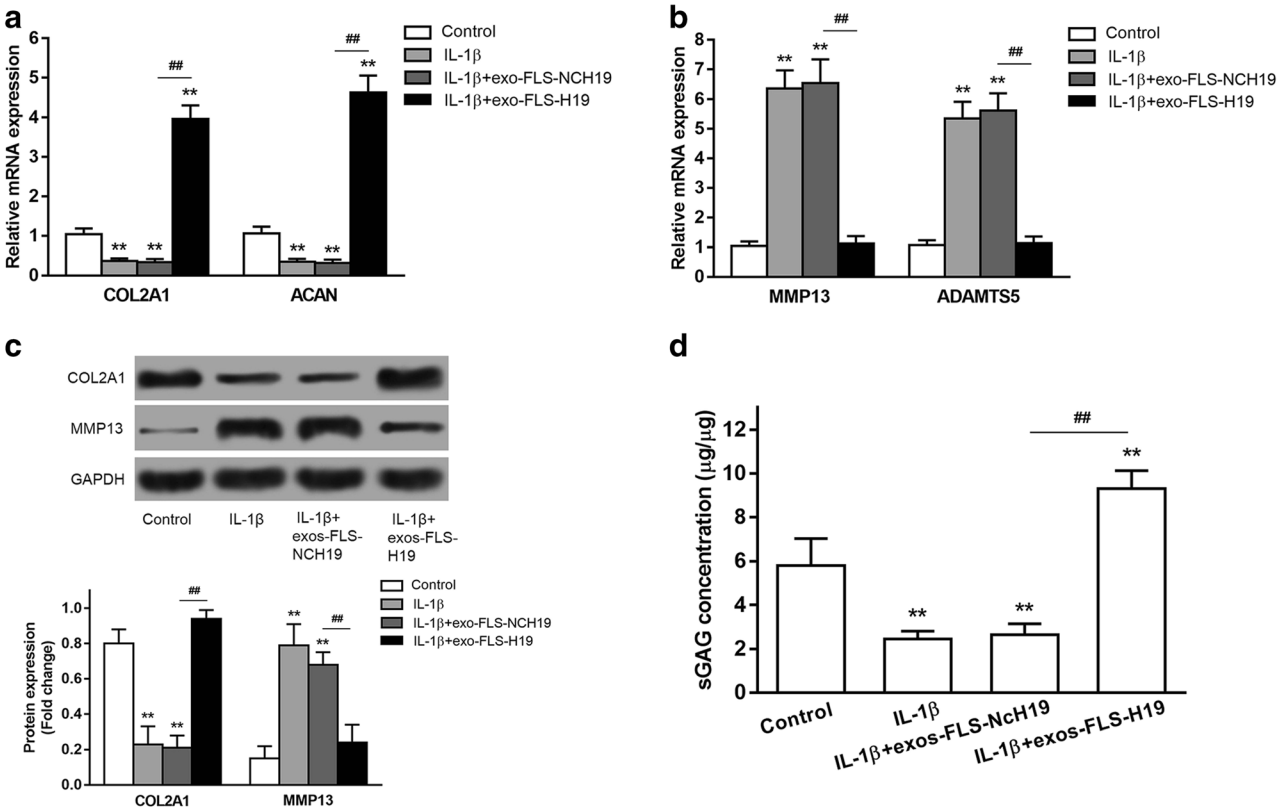

Fig. 4. Exos-FLS-H19 treatment altered ECM degeneration-related molecules of articular chondrocytes. **a** and **b** The expression of mRNA for COL2A1, aggrecan, MMP13, and ADAMTS5 was determined after incubation with exos-FLS-H19, exos-FLS-NCH19 pretreated with10 ng/mL IL-1β for 24 h. **c** The protein expression of type II collagen (COL II) and MMP13 was analyzed by Western blotting after incubation with exos-FLS-H19, exos-FLS-NCH19 pretreated with10 ng/mL IL-1β for 24 h. GAPDH was used as loading control. **d** The levels of sulfated glycosaminoglycan (sGAG) in cell suspensions were assessed by the dimethylmethylene blue assay after incubation with exos-FLS-H19, exos-FLS-NCH19 pretreated with10 ng/mL IL-1β for 24 h. Results were normalized to the total dsDNA content of the cell lysate in each group. Values are the mean ± SEM. $^{*}P < 0.05$, $^{**}P < 0.01$ *vs.* control group, $^{\#\#\#}P < 0.001$ *vs.* IL-1β group

downregulated miR-106b-5p levels may lead to the aberrant overexpression of TIMP2 in chondrocytes (Fig. 6a). Furthermore, luciferase activity was significantly ($P < 0.01$) decreased in chondrocytes co-transfected with a miR-106b-5p mimic and pmirGLO-TIMP2-Wt when compared with cells co-transfected with a miR-106b-5p mimic and pmirGLO-TIMP2-Mut (Fig. 6b). It was observed the miR-106b-5p + TIMP2 group significantly ($P < 0.01$) increased COL2A1 and ACAN expression levels, as well as reduced MMP13 and ADAMTS5 expression, when compared with the miR-106b-5p + vehicle group (Fig. 6c and d). Collectively, these results indicate that the balance between ECM anabolism and catabolism in primary chondrocytes was disrupted when transfected with miR-106b-5p mimics, and this negative effect was reversed *in vitro* by the overexpression of TIMP2.

DISCUSSION

vOA is a chronic, degenerative joint disease characterized by articular cartilage destruction. Even though studies have shown that chondrocytes and FLSs in the synovial lining layer play crucial roles in the degradation of cartilage in OA patients [30, 31], few studies analyzed the interaction between chondrocytes and FLSs in OA pathology [11, 12]. Thus, the present study investigated the effects and the underlying mechanisms of FLSs on phenotypic changes and ECM degradation in chondrocytes. In this study, FLS-exos facilitated chondrocyte proliferation and migration, which is currently considered a main strategy to prevent and control OA [32]. Furthermore, the therapeutic effects of FLS-exos on OA are associated with exosomal lncRNA H19,

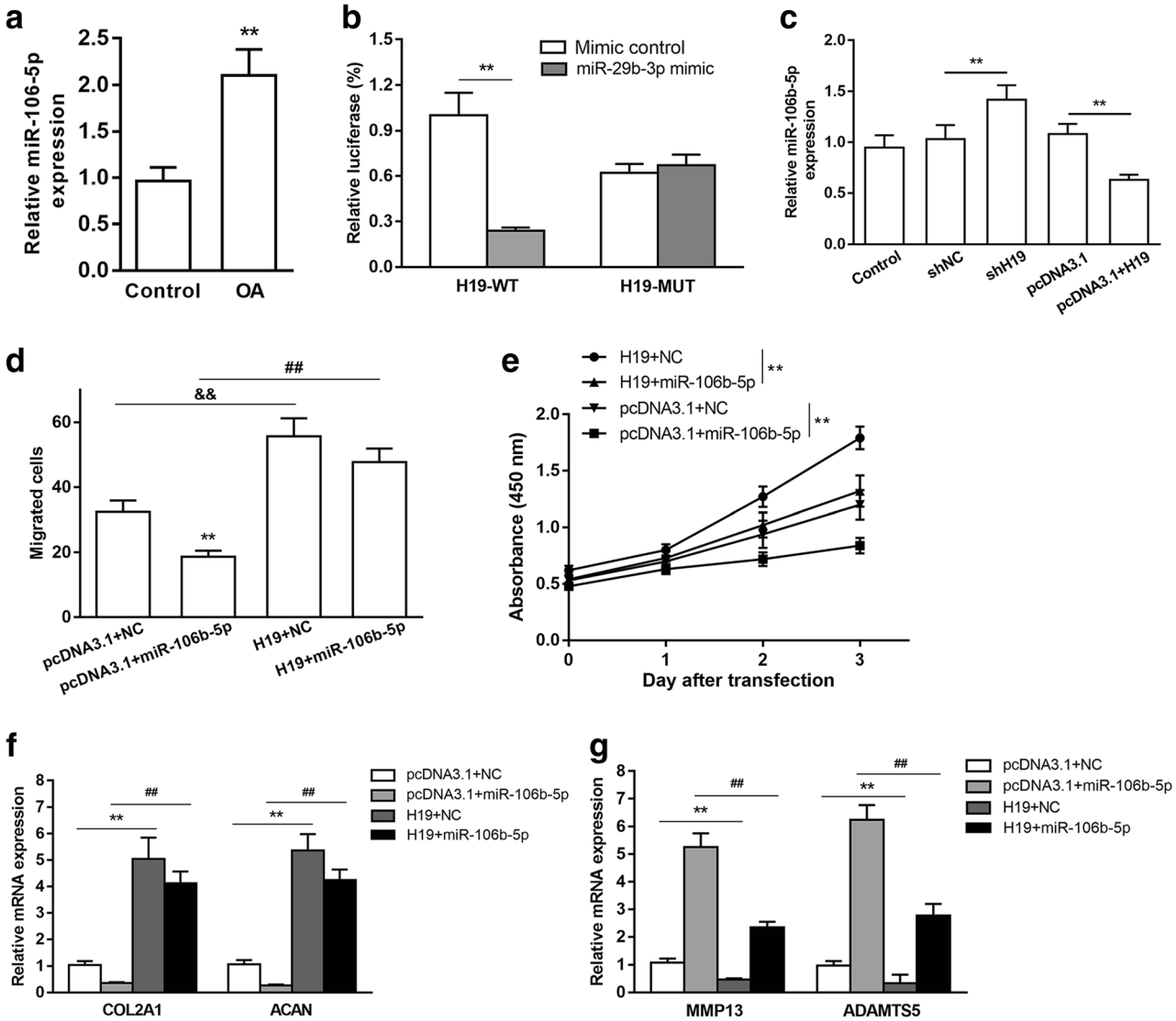

Fig. 5. H19 regulates proliferation, migration, and ECM degradation of chondrocytes *via* targeting miR-106b-5p. **a** Luciferase activities in chondrocytes were compared between miR-106b-5p mimic+H19-WT and miR-106b-5p mimic+H19-MUT groups. $^{***}P < 0.001$ *vs.* mimic control+H19-WT group. **b** Effects of H19 on miR-106b-5p expression were determined in chondrocytes. $^{**}P < 0.01$ *vs.* shNC or pcDNA3.1. **c** The quantitative results of chondrocyte migration determined by transwell experiment are shown. $^{*}P < 0.05$ *vs.* pcDNA3.1 + NC, $^{\#\#}P < 0.01$ *vs.* pcDNA3.1+ miR-106b-5p. **d** Cell Counting Kit-8 assays were performed to determine the proliferative capacity and viability of chondrocytes among H19 + NC, H19 + miR-106b-5p, pcDNA3.1 + NC, pcDNA3.1 + miR-106b-5p groups. $^{*}P < 0.05$. **e** and **f** The expression of mRNA for COL2A1, aggrecan (**e**), MMP13, and ADAMTS5 (**f**) was determined in H19 + NC, H19 + miR-106b-5p, pcDNA3.1 + NC, pcDNA3.1 + miR-106b-5p groups. $^{**}P < 0.01$ *vs.* pcDNA3.1 + NC group, $^{\#\#}P < 0.01$ *vs.* pcDNA3.1 + miR-106b-5p group

which acts as a sponge for miR-106b-5p to promote the expression of TIMP2 in chondrocytes. Exosomes derived from mesenchymal stem cells and synovial fibroblasts mediate cartilage repair by enhancing proliferation, attenuating apoptosis, and balancing the synthesis and degradation of cartilage ECM [33–35]. Our study demonstrated that FLSs-H19-Exos exerted therapeutic effects on OA.

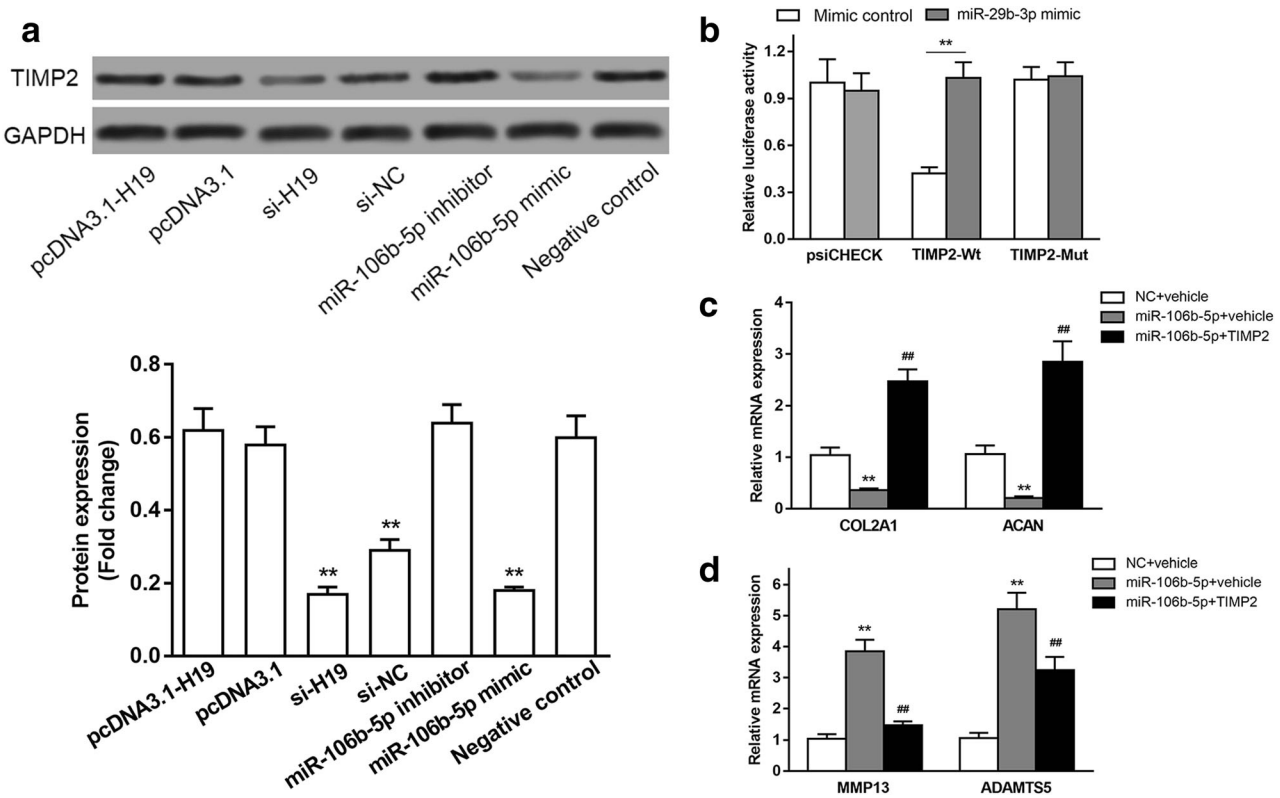

Fig. 6. TIMP2 is a potential target of miR-106b-5p in chondrocytes. **a** TIMP2 expression in pcDNA3.1-H19-, pcDNA3.1-, si-H19-, si-NC-, miR-106bb-5p inhibitor-, miR-106b-5p mimic-, and negative control-transfected chondrocytes. **b** The luciferase activities of chondrocytes were compared between miR-106b-5p mimic + TIMP-Wt and miR-106b-5p mimic + TIMP2-Mut groups. $^{*}P < 0.05$ *vs.* miR-29b-3p mimic + TIMP2-Mut group. **c**–**d** The expression of mRNA for COL2A1, aggrecan (**c**), MMP13, and ADAMTS5 (**d**) was determined among miR-NC + vehicle, miR-29b-3p mimic + vehicle and miR-29b-3p mimic + TIMP2 groups. $^{**}P < 0.01$ *vs.* miR-NC + vehicle group, $^{\#}P < 0.05$, $^{\#\#}P < 0.01$ *vs.* miR-29b-3p mimic + vehicle group

A variety of studies have reported an association between lncRNAs and OA progression [36–38]. Abnormally expressed lncRNAs are associated with both the occurrence and development of OA. To examine potential mediators responsible for the interaction between FLSs and chondrocytes, we investigated the functional correlations between chondrocytes and specific lncRNAs. Previous work [23] has demonstrated that H19 overexpression induces ECM synthesis, which is considered a compensatory mechanism used by chondrocytes to counteract matrix destruction during OA, by targeting miR-675. However, a different study [39] suggests that H19 exerts stimulatory effects on cell damage of normal human cartilage cells C28/I2 by targeting miR-130a. These conflicting findings may partly be due to the different origins of chondrocytes. Our data suggested that the lncRNA H19 may be involved in the protective effects of FLS-exos on OA.

LncRNAs are considered molecules in regulating diverse biological processes by serving as molecular sponges for specific miRNAs. The miR-106b-5p has regulatory roles in various cell types. For example, miR-106b-5p was shown to inhibit the invasion and metastasis of colorectal cancer by targeting CTSA [40]. Targeting PTEN through miR-106b-5p promotes stem cell-like properties of hepatocellular carcinoma cells [41]. In inflammatory diseases, a miR-106b-5p antagomir protects against cerebral ischemia/reperfusion (I/R) injury [42]. Also, miR-106b-5p is associated with inflammatory responses and bone destruction in collagen-induced arthritis [43]. Our work showed that H19 protects against IL-1β-induced chondrocyte damage by interacting with miR-106b-5p.

Furthermore, we identified TIMP2 as a miR-106b-5p target in OA development. TIMP2, a member of the TIMP family, plays a regulatory role in the proteolytic activities

of MMPs. However, the MMP inhibitory capacity of TIMPs appears low in OA cartilage [44]. In addition, the introduction of exogenous TIMPs to suppress the overactivity of MMPs in OA joints showed little clinical effects [45]. Our findings confirmed the regulating role of TIMP2 in the synthesis and degradation of the ECM. However, the detailed mechanisms by which TIMP2 balances ECM anabolism and catabolism in articular chondrocytes require further investigation.

In conclusion, our work demonstrates an axis explaining the role of the lncRNA H19 in OA development. FLS-derived exosomal lncRNA H19 promotes cell viability and migration, and protects against ECM degradation in IL-1-β-induced chondrocytes by regulating miR-106b-5p and TIMP2 expression. These findings highlight a novel pathological mechanism for OA, underling a possible therapeutic target for OA.

REFERENCES

1. Guermazi, A., F.W. Roemer, D. Burstein, and D. Hayashi. 2011. Why radiography should no longer be considered a surrogate outcome measure for longitudinal assessment of cartilage in knee osteoarthritis. *Arthritis Research & Therapy* 13: 247.
2. Pan, L., Y. Zhang, N. Chen, and L. Yang. 2017. Icariin regulates cellular functions and gene expression of osteoarthritis patient-derived human fibroblast-like synoviocytes. *International Journal of Molecular Sciences* 18.
3. Pelletier, J.P., J. Martel-Pelletier, and S.B. Abramson. 2001. Osteoarthritis, an inflammatory disease: potential implication for the selection of new therapeutic targets. *Arthritis and Rheumatism* 44: 1237–1247.
4. Krenn, V., L. Morawietz, G.R. Burmester, R.W. Kinne, U. Mueller-Ladner, B. Muller, and T. Haupl. 2006. Synovitis score: discrimination between chronic low-grade and high-grade synovitis. *Histopathology* 49: 358–364.
5. Ding, X., Y. Zhang, Y. Huang, S. Liu, H. Lu, and T. Sun. 2015. Cadherin-11 involves in synovitis and increases the migratory and invasive capacity of fibroblast-like synoviocytes of osteoarthritis. *International Immunopharmacology* 26: 153–161.
6. Nair, A., V. Kanda, C. Bush-Joseph, N. Verma, S. Chubinskaya, K. Mikecz, T.T. Glant, A.M. Malfait, M.K. Crow, G.T. Spear, A. Finnegan, and C.R. Scanzello. 2012. Synovial fluid from patients with early osteoarthritis modulates fibroblast-like synoviocyte responses to toll-like receptor 4 and toll-like receptor 2 ligands via soluble cd14. *Arthritis and Rheumatism* 64: 2268–2277.
7. Kloesch, B., M. Liszt, D. Krehan, J. Broell, H. Kiener, and G. Steiner. 2012. High concentrations of hydrogen sulphide elevate the expression of a series of pro-inflammatory genes in fibroblast-like synoviocytes derived from rheumatoid and osteoarthritis patients. *Immunology Letters* 141: 197–203.
8. Fu, Z., P. Liu, D. Yang, F. Wang, L. Yuan, Z. Lin, and J. Jiang. 2012. Interleukin-18-induced inflammatory responses in synoviocytes and chondrocytes from osteoarthritic patients. *International Journal of Molecular Medicine* 30: 805–810.
9. Fernandes, J.C., J. Martel-Pelletier, and J.P. Pelletier. 2002. The role of cytokines in osteoarthritis pathophysiology. *Biorheology* 39: 237–246.
10. Hasegawa, A., H. Nakahara, M. Kinoshita, H. Asahara, J. Koziol, and M.K. Lotz. 2013. Cellular and extracellular matrix changes in anterior cruciate ligaments during human knee aging and osteoarthritis. *Arthritis Research & Therapy* 15: R29.
11. Steenvoorden, M.M., R.A. Bank, H.K. Ronday, R.E. Toes, T.W. Huizinga, and J. DeGroot. 2007. Fibroblast-like synoviocyte-chondrocyte interaction in cartilage degradation. *Clinical and Experimental Rheumatology* 25: 239–245.
12. Huh, Y.H., G. Lee, W.H. Song, J.T. Koh, and J.H. Ryu. 2015. Crosstalk between FLS and chondrocytes is regulated by HIF-2alpha-mediated cytokines in arthritis. *Experimental & Molecular Medicine* 47: e197.
13. Cui, Z., S. Ren, J. Lu, F. Wang, W. Xu, Y. Sun, M. Wei, J. Chen, X. Gao, C. Xu, J.H. Mao, and Y. Sun. 2013. The prostate cancer-up-regulated long noncoding RNA plncrna-1 modulates apoptosis and proliferation through reciprocal regulation of androgen receptor. *Urologic Oncology* 31: 1117–1123.
14. Akhtar, N., Z. Rasheed, S. Ramamurthy, A.N. Anbazhagan, F.R. Voss, and T.M. Haqqi. 2010. Microrna-27b regulates the expression of matrix metalloproteinase 13 in human osteoarthritis chondrocytes. *Arthritis and Rheumatism* 62: 1361–1371.
15. Nugent, M. 2016. MicroRNAs: exploring new horizons in osteoarthritis. *Osteoarthritis and Cartilage* 24: 573–580.
16. Gupta, R.A., N. Shah, K.C. Wang, J. Kim, H.M. Horlings, D.J. Wong, M.C. Tsai, T. Hung, P. Argani, J.L. Rinn, Y. Wang, P. Brzoska, B. Kong, R. Li, R.B. West, M. van de Vijver, S. Sukumar, and H.Y. Chang. 2010. Long non-coding RNA HOTAIR reprograms chromatin state to promote cancer metastasis. *Nature* 464: 1071–1076.
17. Chang, T., J. Xie, H. Li, D. Li, P. Liu, and Y. Hu. 2016. MicroRNA-30a promotes extracellular matrix degradation in articular cartilage via downregulation of Sox9. *Cell Proliferation* 49: 207–218.
18. Wu, J., M. Zou, A. Ping, Z. Deng, and L. Cai. 2018. MicroRNA-449a upregulation promotes chondrocyte extracellular matrix degradation in osteoarthritis. *Biomedicine & Pharmacotherapy* 105: 940–946.
19. Li, Y.F., S.H. Li, Y. Liu, and Y.T. Luo. 2017. Long noncoding RNA CIR promotes chondrocyte extracellular matrix degradation in osteoarthritis by acting as a sponge for Mir-27b. *Cellular Physiology and Biochemistry* 43: 602–610.
20. Sun, H., G. Wang, Y. Peng, Y. Zeng, Q.N. Zhu, T.L. Li, J.Q. Cai, H.H. Zhou, and Y.S. Zhu. 2015. H19 lncRNA mediates 17beta-estradiol-induced cell proliferation in MCF-7 breast cancer cells. *Oncology Reports* 33: 3045–3052.
21. Lv, J., Y.Q. Yu, S.Q. Li, L. Luo, and Q. Wang. 2014. Aflatoxin b1 promotes cell growth and invasion in hepatocellular carcinoma HepG2 cells through h19 and e2f1. *Asian Pacific Journal of Cancer Prevention* 15: 2565–2570.
22. Liu, C., Z. Chen, J. Fang, A. Xu, W. Zhang, and Z. Wang. 2016. H19-derived miR-675 contributes to bladder cancer cell proliferation by regulating p53 activation. *Tumour Biology* 37: 263–270.
23. Steck, E., S. Boeuf, J. Gabler, N. Werth, P. Schnatzer, S. Diederichs, and W. Richter. 2012. Regulation of h19 and its encoded microRNA-675 in osteoarthritis and under anabolic and catabolic in vitro conditions. *Journal of Molecular Medicine (Berlin, Germany)* 90: 1185–1195.

24. Fattahi, M., N. Rezaei, F.S. Nematalahi, V. Shaygannejad, S. Fouladi, L. Karimi, F. Fathi, L. Dehghani, O. Mirmosayyeb, and N. Eskandari. 2019. MicroRNA-29b variants and MxA expression change during interferon beta therapy in patients with relapsing-remitting multiple sclerosis. *Multiple Sclerosis and Related Disorders* 35: 241–245.
25. Tao, R., X.X. Fan, H.J. Yu, G. Ai, H.Y. Zhang, H.Y. Kong, Q.Q. Song, Y. Huang, J.Q. Huang, and Q. Ning. 2018. MicroRNA-29b-3p prevents Schistosoma japonicum-induced liver fibrosis by targeting COL1A1 and COL3A1. *Journal of Cellular Biochemistry* 119: 3199–3209.
26. Vandooren, B., T. Cantaert, M. ter Borg, T. Noordenbos, R. Kuhlman, D. Gerlag, T. Bongartz, K. Reedquist, P.P. Tak, and D. Baeten. 2008. Tumor necrosis factor alpha drives cadherin 11 expression in rheumatoid inflammation. *Arthritis and Rheumatism* 58: 3051–3062.
27. Gosset, M., F. Berenbaum, S. Thirion, and C. Jacques. 2008. Primary culture and phenotyping of murine chondrocytes. *Nature Protocols* 3: 1253–1260.
28. Qin, J., L. Shang, A.S. Ping, J. Li, X.J. Li, H. Yu, J. Magdalou, et al. 2012. TNF/TNFR signal transduction pathway-mediated anti-apoptosis and anti-inflammatory effects of sodium ferulate on Il-1beta-induced rat osteoarthritis chondrocytes in vitro. *Arthritis Research & Therapy* 14: R242.
29. Zhang, G., Y. Sun, Y. Wang, R. Liu, Y. Bao, and Q. Li. 2016. MiR-502-5p inhibits Il-1beta-induced chondrocyte injury by targeting TRAF2. *Cellular Immunology* 302: 50–57.
30. Firestein, G.S. 1996. Invasive fibroblast-like synoviocytes in rheumatoid arthritis. Passive responders or transformed aggressors? *Arthritis and Rheumatism* 39: 1781–1790.
31. Neidhart, M., C.A. Seemayer, K.M. Hummel, B.A. Michel, R.E. Gay, and S. Gay. 2003. Functional characterization of adherent synovial fluid cells in rheumatoid arthritis: destructive potential in vitro and in vivo. *Arthritis and Rheumatism* 48: 1873–1880.
32. Hu, W., W. Zhang, F. Li, F. Guo, and A. Chen. 2016. MiR-139 is up-regulated in osteoarthritis and inhibits chondrocyte proliferation and migration possibly via suppressing EIF4G2 and IGF1R. *Biochemical and Biophysical Research Communications* 474: 296–302.
33. Zhang, S., S.J. Chuah, R.C. Lai, J.H.P. Hui, S.K. Lim, and W.S. Toh. 2018. MSC exosomes mediate cartilage repair by enhancing proliferation, attenuating apoptosis and modulating immune reactivity. *Biomaterials* 156: 16–27.
34. Kato, T., S. Miyaki, H. Ishitobi, Y. Nakamura, T. Nakasa, M.K. Lotz, and M. Ochi. 2014. Exosomes from Il-1beta stimulated synovial fibroblasts induce osteoarthritic changes in articular chondrocytes. *Arthritis Research & Therapy* 16: R163.
35. Wang, Y., D. Yu, Z. Liu, F. Zhou, J. Dai, B. Wu, J. Zhou, et al. 2017. Exosomes from embryonic mesenchymal stem cells alleviate osteoarthritis through balancing synthesis and degradation of cartilage extracellular matrix. *Stem Cell Research & Therapy* 8: 189.
36. Li, Y., S. Li, Y. Luo, Y. Liu, and N. Yu. 2017. LncRNA PVT1 regulates chondrocyte apoptosis in osteoarthritis by acting as a sponge for miR-488-3p. *DNA and Cell Biology* 36: 571–580.
37. Dang, X., L. Lian, and D. Wu. 2018. The diagnostic value and pathogenetic role of lncRNA-ATB in patients with osteoarthritis. *Cellular & Molecular Biology Letters* 23: 55.
38. Xu, J., and Y. Xu. 2017. The lncRNA MEG3 downregulation leads to osteoarthritis progression via miR-16/SMAD7 axis. *Cell & Bioscience* 7: 69.
39. Hu, Y., S. Li, and Y. Zou. 2019. Knockdown of lncRNA h19 relieves LPS-induced damage by modulating miR-130a in osteoarthritis. *Yonsei Medical Journal* 60: 381–388.
40. Ni, S., W. Weng, M. Xu, Q. Wang, C. Tan, H. Sun, L. Wang, D. Huang, X. du, and W. Sheng. 2018. MiR-106b-5p inhibits the invasion and metastasis of colorectal cancer by targeting CTSA. *Onco Targets Ther* 11: 3835–3845.
41. Shi, D.M., X.Y. Bian, C.D. Qin, and W.Z. Wu. 2018. MiR-106b-5p promotes stem cell-like properties of hepatocellular carcinoma cells by targeting PTEN via PI3K/Akt pathway. *Onco Targets Ther* 11: 571–585.
42. Li, P., M. Shen, F. Gao, J. Wu, J. Zhang, F. Teng, and C. Zhang. 2017. An antagomir to microRNA-106b-5p ameliorates cerebral ischemia and reperfusion injury in rats via inhibiting apoptosis and oxidative stress. *Molecular Neurobiology* 54: 2901–2921.
43. Tao, Y., Z. Wang, L. Wang, J. Shi, X. Guo, W. Zhou, X. Wu, Y. Liu, W. Zhang, H. Yang, Q. Shi, Y. Xu, and D. Geng. 2017. Downregulation of miR-106b attenuates inflammatory responses and joint damage in collagen-induced arthritis. *Rheumatology (Oxford)* 56: 1804–1813.
44. Meszaros, E., and C.J. Malemud. 2012. Prospects for treating osteoarthritis: enzyme-protein interactions regulating matrix metalloproteinase activity. *Ther Adv Chronic Dis* 3: 219–229.
45. Clutterbuck, A.L., K.E. Asplin, P. Harris, D. Allaway, and A. Mobasheri. 2009. Targeting matrix metalloproteinases in inflammatory conditions. *Current Drug Targets* 10: 1245–1254.